Plasma Scenario Study for HT-6 M Tokamak Using BALDUR Integrated Predictive Modeling Code*)

Jiraporn PROMPING[1)], Siriyaporn SANGAROON[2)], Apiwat WISITSORASAK[3,4)], Boonyarit CHATTHONG[5)], Roppon PICHA[1)] and Thawatchai ONJUN[1)]

[1)] *Thailand Institute of Nuclear Technology, Bangkok, Thailand*
[2)] *Department of Physics, Mahasarakham University, Mahasarakham, Thailand*
[3)] *Department of Physics, Faculty of Science, King Mongkut University of Technology Thonburi, Bangkok, Thailand*
[4)] *Theoretical and Computational Physics Group, Theoretical and Computational Science Center, King Mongkut University of Technology Thonburi, Bangkok, Thailand*
[5)] *Department of Physics, Faculty of Science, Prince of Songkla University, Songkla, Thailand*

(Received 28 December 2017 / Accepted 5 June 2018)

This study investigates the plasma performance in HT-6 M tokamak using 1.5D integrated predictive modeling code BALDUR. The simulations are carried out under the designed plasma conditions, including $R = 65$ cm, $a = 20$ cm, $B_T = 1.5$ T, $n_e = 1 \times 10^{19}$ m^{-3} and $I_p = 40$ - 150 kA without external heating. In these simulations, a combination of turbulence and neoclassical transports is used for predicting thermal and particle transport. Thus, the plasma evolution for plasma current, temperature, and density can be predicted under a designed condition. In addition, the influence of current rampup for the plasma performanceis investigated. The scenario study for the tokamak is also carried out by varying plasma current. To summarize the results yield the electron temperature at the center $T_e(0) = 477$ - 1,551 eV (MMM95) and 328 - 1,384 eV (Mixed B/gB), the ion temperature at the center $T_i(0) = 26$ - 50 eV (MMM95) and 18 - 42 eV (Mixed B/gB) the electron densit $y = 6.4 \times 10^{18}$ - 1.4×10^{19} m^{-3} in both Mixed B/gB and MMM95 simulations. Using the obtained plasma parameters, the radiated power of the carbon impurity is assessed.

Keywords: tokamak, plasma, BALDUR, transport, MMM95, Mixed B/gB

DOI: 10.1585/pfr.13.3403094

1. Introduction

The prediction of plasma performance in a tokamak can be achieved in the nuclear fusion community by using integrated predictive modeling codes to compute the time evolution of plasma profiles such as temperature and density. This task has been done using various integrated predictive modeling codes, for example BALDUR [1], TASK [2], JETTO [3], CRONOS [4] and ASTRA [5]. Cross-comparison between the predictions of different codes is important for the research in order to improve our confidence on these codes predictive capability [6,7]. Moreover, it is known that plasma performance in a tokamak depends on many parameters. Therefore, the purpose of this paper is to compare plasma performance as the plasma parameters are varied; example of these quantities is plasma current. In this work, BALDUR code is used with two different core transport models Multi mode model (MMM95) [8] and Mixed Bohm/gyro-Bohm (Mixed B/gB) model [9]. The neoclassical transport is calculated using NCLASS model [10].

The simulations are carried out with plasma parameters based on the HT-6 M tokamak (formerly developed and operated by ASIPP, China) [11] which allows us to predict the transport behavior and compare with the existing experimental results [11]. The total radiation is then calculated using the ADAS database [12] via the global spectral line and continuum radiative coefficient. The simulations provide an understanding of plasma behavior in the HT-6 M experiment.

This paper is organized as follows: brief descriptions of BALDUR integrated predictive modeling code, Turbulent Transport Models (Multi mode model and Mixed Bohm/gyro-Bohm), are given in the next section. In section 3, the simulation results are shown and the previous experiment results [11] are compared. Section 4 summarizes this study.

2. Simulation Method

Basically, an integrated predictive modeling code is a collection of several modules containing different physics, such as a neutral beam heating module, an RF heating module, a core transport module, and an impurity radiation module, in which each module is responsible for its own specific tasks. These modules are solved self-consistently

author's e-mail: jirapornp@tint.or.th

*) This article is based on the presentation at the 26th International Toki Conference (ITC26).

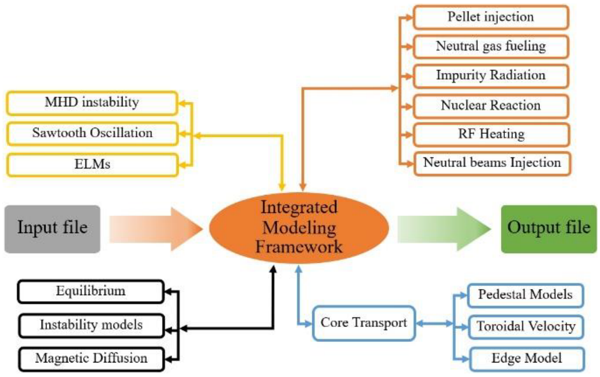

Fig. 1 The framework of BALDUR code.

with one another. In general, the input data needed for an integrated predictive modeling code is the controlled plasma parameters in experiments, such as magnetic field, total heating power, and plasma current. With these plasma parameters, a time evolution of plasma simulations is carried out according to the selected modules.

2.1 BALDUR code

BALDUR is an integrated predictive modeling code developed to compute the time evolution of plasma profiles including electron and ion temperatures, deuterium, tritium, helium and impurity densities, safety factor q, neutrals, and fast ions. These time-evolving profiles are computed by including the effects of transport, plasma heating, particle influx, boundary conditions, the plasma equilibrium shape, and sawtooth oscillations. Fusion heating power and helium ash accumulation are also computed self-consistently. The BALDUR simulations have been intensively compared against various plasma experiments, which yield agreement with 10 % relative RMS deviation as described in Refs [13, 14]. The flowchart of BALDUR is shown in Fig. 1.

2.2 Turbulent transport models

In this work, two turbulent transport models are used: the MMM95 and Mixed B/gB model. Brief descriptions of the models are given as follows.

2.2.1 Multi-mode model

The Multi-Mode Model version 1995 (MMM95) is a combination of theory-motivated transport models used to predict the temperature and density of plasma profiles in tokamaks [8, 15, 16]. It consists of the Weliand model for the ion temperature gradient (ITG) and trapped electron modes (TEM) [17, 18], the Guzdar-Drake model for drift-resistive ballooning modes (RB) [19], and kinetic ballooning modes (KB) [8]. The linear combination of transport coefficients in MMM95 can be expressed as:

$$\chi_i = 0.8\chi_{i,1TG\&TEM} + \chi_{i,RB} + \chi_{i,KB}, \tag{1}$$

$$\chi_e = 0.8\chi_{i,1TG\&TEM} + \chi_{e,RB} + \chi_{e,KB}, \tag{2}$$

$$D_H = 0.8D_{H,1TG\&TEM} + \chi_{H,RB} + \chi_{H,KB}, \tag{3}$$

$$D_z = 0.8D_{z,1TG\&TEM} + \chi_{z,RB} + \chi_{z,KB}, \tag{4}$$

where χ_i and χ_e are the ion and electron thermal transport coefficients, respectively, D_H is the particle transport coefficients, D_z is the impurity diffusivity, $\chi_{1TG\&TEM}$ is the thermal diffusivity of the ion temperature gradient and trapped-electron mode, χ_{RB} is the resistive ballooning thermal diffusivity, and χ_{KB} is the kinetic ballooning thermal diffusivity. All the anomalous transport contributions to the MMM95 transport model are multiplied by the inverse forth power of the local elongation (κ^{-4}) since the models were originally derived for circular plasmas [8]. This would allow the simulations to produce the observed asymptotic scaling of the confinement time which increases with the elongation κ at constant q and β as $\tau_e \propto I_p^2/(nT) \propto (1+k^2)^2/(q^2\beta)$.

2.2.2 Mixed Bohm/gyro Bohm

The Mixed B/gB core transport model is an empirical transport model. It was originally a local transport model with Bohm scaling. A transport model is said to be "local" if the transport fluxes (such as heat and particle fluxes) depend entirely on local plasma properties (such as temperatures, densities, and their gradients). The Mixed B/gB transport model can be expressed as follows [20]:

$$\chi_i = 0.5\chi_{gB} + 0.4\chi_B, \tag{5}$$

$$\chi_e = 1.0\chi_{gB} + 2.0\chi_B, \tag{6}$$

$$D_H = D_z = (0.3 + 0.7\rho)\frac{\chi_e\chi_i}{\chi_e + \chi_i}, \tag{7}$$

where χ_i and χ_e are the ion and electron diffusivity, respectively, D_H and D_z are the particle and impurity diffusivity, respectively, ρ is the normalized minor radius.

The Bohm term [21, 22] and Gyro-Bohm term [23] can be expressed as follows:

$$\chi_{gB} = 5\times 10^{-6}\sqrt{T_e}\left|\frac{\nabla T_e}{B_T^2}\right|, \tag{8}$$

$$\chi_B = \chi_{B_0}\times\Theta\left(-0.14 + s - \frac{1.47\omega_{E\times B}}{\gamma_{ITG}}\right), \tag{9}$$

with

$$\chi_{B_0} = 4\times 10^{-5}R\left|\frac{\nabla(n_eT_e)}{n_eB_\phi}\right|q^2 \times\left(\frac{T_e(0.8\rho_{max}) - T_e(\rho_{max})}{T_e(\rho_{max})}\right), \tag{10}$$

where χ_{gB} is the gyro-Bohm contribution, T_e is the local electron temperature in keV, B_T is the toroidal magnetic field, χ_B is the Bohm contribution, s is the magnetic shear, $\omega_{E\times B}$ is the shearing rate, γ_{ITG} is the linear growth rate, R is the major radius, n_e and is the local electron density.

The Hahm-Burrell shearing rate $\omega_{E\times B}$ can be calculated as [24, 25]:

$$\omega_{E\times B} = \left|\frac{RB_\theta^2}{B_T}\frac{(E_r/RB_\theta)}{\partial\psi}\right|, \tag{11}$$

where B_θ is poloidal magnetic field, Ψ is the poloidal flux and E_r is the profiles of radial electric field with obtained from the poloidal and toroidal velocity, respectively.

2.3 Radiation Power

To understand the impurity behavior in HT-6 M tokamak, a global model of total radiated power profile has been developed using the ADAS database under the assumption of the steady-state plasma conditions. The spatial density distribution of all ionization stages of carbon are then calculated with prescribed neoclassical and turbulent transport coefficients [12]. The carbon impurity radiation is computed using a collisional-radiative model including the effect of electron collisional ionisation and excitation, spontaneous decay (so-called spectral line radiation) and recombination cascade and bremsstrahlung (so-called continuum radiation).

3. Results and Discussion

HT-6 M is a small-sized tokamak with circular cross section, R = 65 cm, a = 20 cm, B_T = 1.5 T, n_e = 1×10^{19} m^{-3} and I_p = 40 - 150 kA. HT-6 M was operated without the external heating power. The boundary conditions in each simulation are set with the same conditions. All simulations are assumed the electron densit $y = 1.0 \times 10^{19}$ m^{-3}. The BALDUR code including turbulent transport models, MMM95 and Mixed B/gB model, are used to carry out the plasma of the HT-6 M.

The electron temperature, ion temperature and electron density profiles are shown in Fig. 2 as functions of normalized minor radius with plasma current varying between 40 - 60 kA. The simulation results of the electron and ion temperatures using MMM95 tend to be higher than those using Mixed B/gB. However, the electron densities from Mixed B/gB appear to be higher. Plasma temperatures increase with higher plasma current. The simulations results are summarized in Table 1 and Fig. 3.

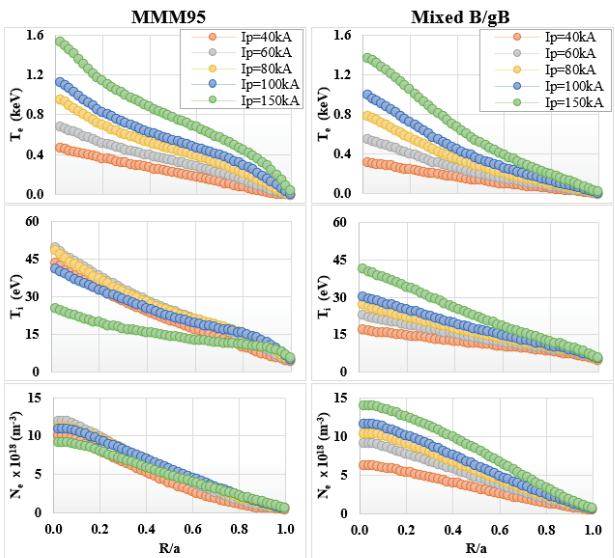

Fig. 2 The profiles of electron temperatures (top), the ion temperature (middle) and electron density (bottom) as functions of normalized minor radius with plasma current varying between 40 - 150 kA.

Table 1 The simulation results of the temperatures and the electron density at the magnetic axis.

	T_e (eV)		T_i (eV)		n_e($\times 10^{18}$m^{-3})	
Model / Ip	MMM	Mixed B/gB	MMM	Mixed B/gB	MMM	Mixed B/gB
40kA	477	328	44	18	10	6
60kA	695	563	50	23	12	9
80kA	967	801	49	28	11	11
100kA	1,138	1,003	42	31	11	12
150kA	1,551	1,384	26	42	9	14

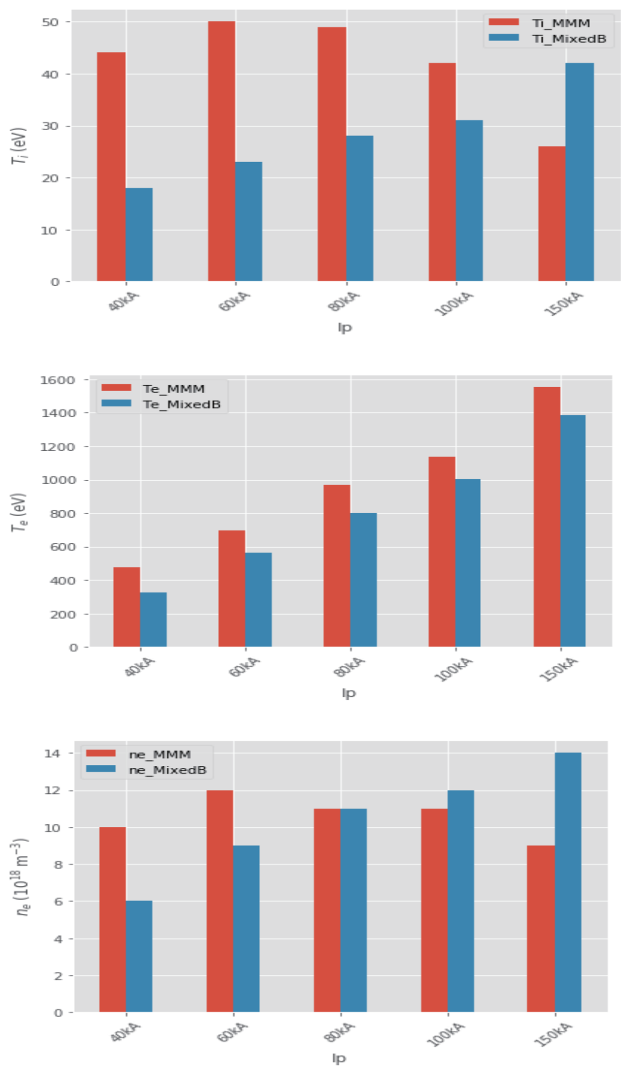

Fig. 3 Ion temperatures, electron temperatures, and electron densities calculated by the two models at different plasma currents.

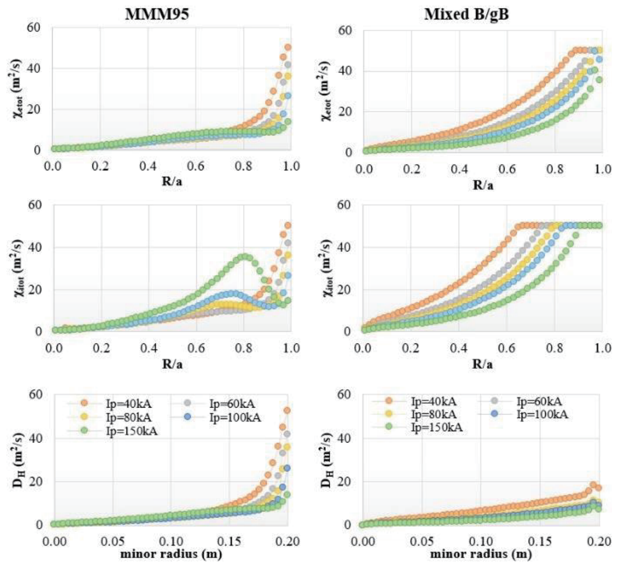

Fig. 4 The profiles of the electron thermal diffusivity (top) and the ion thermal diffusivity (middle) as functions of normalized minor radius and the particle diffusion coefficients of hydrogen (bottom) as functions of normalized minor radius with plasma current between 40 - 150 kA.

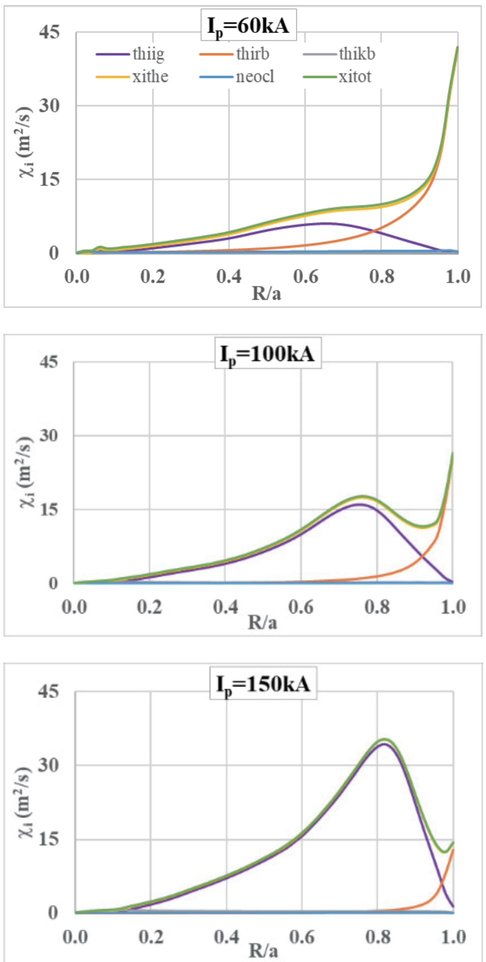

Fig. 5 The profiles of the ion thermal diffusivity with I_p = 60 kA (top), I_p = 100 kA (middle) and I_p = 150 kA (bottom) as functions of normalized.

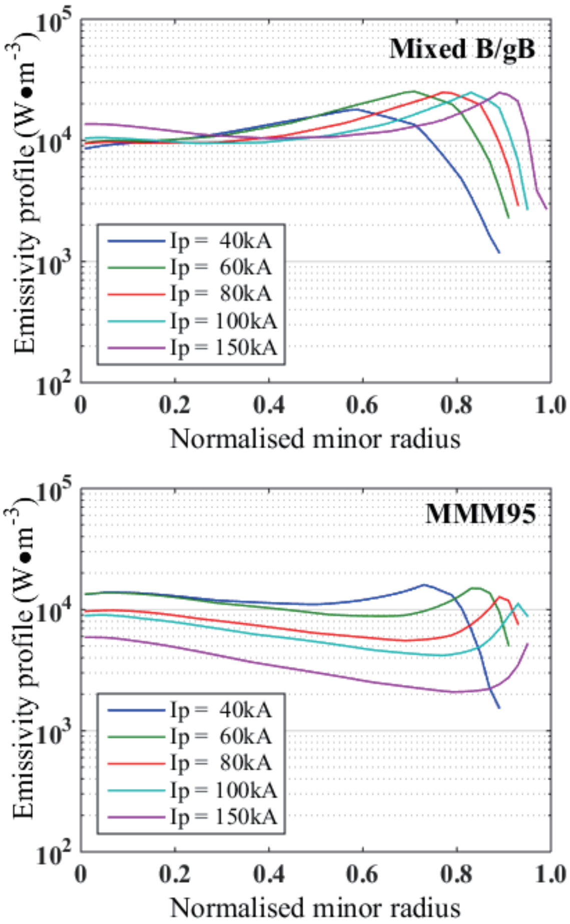

Fig. 6 Profiles of the carbon power radiation as functions of normalized minor radius for Mixed B/gB (top) and MMM95 (bottom).

We also found that the calculated diffusivity is dominant in small regions closed to the edge. But at the plasma core, the total electron thermal diffusivities from simulations using Mixed B/gB model are higher than those using MMM95 model (Fig. 4). Particle diffusion coefficient of hydrogen calculated from Mixed B/gB model are significantly higher than those from MMM95 model.

It can be observed from Fig. 5 that the ion thermal diffusivity of simulation using I_p = 150 kA appears to have a large peak value at R/a = 0.8. At ITG is a dominant term in MMM95 model, this peaking behaviour results in decrease in ion temperature.

HT-6 M was originally designed for the study of transport process and diffusion process of impurity [11]. An ideal impurity transport code has been used to simulate impurities (carbon and oxygen) behaviour during the OH discharge [26]. This work aims to study the scenario with hydrogen plasmas with carbon as impurity species. Despite the all-metal first wall, carbon was found to be the major low-Z impurity in tokamaks during operation, especially in small and medium-sized devices. Thus, the prediction of intrinsic carbon penetrating into the main plasma and its effect on the plasma itself must be assessed. As shown in Fig. 6, the calculated radiation power from Mixed B/gB transport model remains nearly constant from the core to the region around $R/a = 0.7$. The radiation power then significantly increases and drops at the edge. For the MMM95 transport model, the radiation power tends to decrease from the core to the region around $R/a = 0.75$ and then slightly increase before decreasing at the edge.

4. Conclusion

Turbulent transport models (Mixed Bohm/gyro-Bohm model and Multi-mode model are used with BALDUR code to calculate plasma profiles for different plasma parameters of HT-6 M tokamak. The results show that the electron temperature at the center $T_e(0) = 477$ - 1,551 eV (MMM95) and 328 - 1,384 eV (Mixed B/gB), the ion temperature at the center $T_i(0) = 26$ - 50 eV (MMM95) and 18 - 42 eV (Mixed B/gB) the electron densit $y = 6.4 \times 10^{18}$ - 1.4×10^{19} m^{-3} in both Mixed B/gB and MMM95 simulations. Moreover, when the plasma current is increased, the electron and ion thermal transports do not increase. Consequently, particle diffusion coefficient of hydrogen and power radiated remain relatively unchanged.

Acknowledgements

This work contributes to the activities of the Center for Plasma and Nuclear Fusion Technology (CPaF), Thailand Institute of Nuclear Technology (Public Organization). This work was partly supported by the International Atomic Energy Agency (IAEA) under Contract No. 22785.

[1] C.E. Singer *et al.*, Comput. Phys. Commun. **49**, 275 (1988).
[2] A. Fukuyama *et al.*, 20th IAEA Fusion Energy Conf. IAEA-CSP-25/CD/TH/P2-3 (2004).
[3] G. Cenacchi and A. Taroni, ENEA-RT-TIB-88-5 19, 19097143 (1988).
[4] J.F. Artaud *et al.*, Nucl. Fusion **50**, 043001 (2010).
[5] G.V. Pereverzev and P.N. Yushmanov, Max-Planck-Institut für Plasmaphysik, Garching, IPP 5/98 (2002).
[6] C.E. Kessel *et al.*, Nucl. Fusion **47**, 1274 (2007).
[7] M. Murakami *et al.*, Nucl. Fusion **51**, 103006 (2011).
[8] G. Bateman *et al.*, Phys. Plasmas **5**, 1793 (1998).
[9] T.J.J. Tala *et al.*, Plasma Phys. Control. Fusion **43**, 507 (2001).
[10] W.A. Houlberg *et al.*, Phys. Plasmas **4**, 3230 (1997).
[11] H.-6 M Team, Fusion Technol. **9**, 476 (1986).
[12] H.P. Summers, The ADAS User Manual, version 2.6 (2004). http://adas.ac.uk
[13] D. Hannum *et al.*, Phys. Plasmas **8**, 964 (2001).
[14] T. Onjun *et al.*, Phys. Plasmas **8**, 975 (2001).
[15] J.E. Kinsey, G. Bateman, A.H. Kritz and A. Redd, Phys. Plasmas **3**, 561 (1996).
[16] J.E. Kinsey and G. Bateman, Phys. Plasmas **3**, 3344 (1996).
[17] H. Nordman, J. Weiland and A. Jarmén, Nucl. Fusion **30**, 983 (1990).
[18] J. Weiland and A. Hirose, Nucl. Fusion **32**, 151 (1992).
[19] P.N. Guzdar, J.F. Drake, D. McCarthy, A.B. Hassam and C.S. Liu, Phys. Fluids B Plasma Phys. **5**, 3712 (1993).
[20] T.J.J. Tala *et al.*, Plasma Phys. Control. Fusion **44**, A495 (2002).
[21] A. Taroni, M. Erba, E. Springmann and F. Tibone, Plasma Phys. Control. Fusion **36**, 1629 (1994).
[22] M. Erba, V. Parail, E. Springmann and A. Taroni, Plasma Phys. Control. Fusion **37**, 1249 (1995).
[23] M. Erba, T. Aniel, V. Basiuk, A. Becoulet and X. Litaudon, Nucl. Fusion **38**, 1013 (1998).
[24] P. Zhu, G. Bateman, A.H. Kritz and W. Horton, Phys. Plasmas **7**, 2898 (2000).
[25] A.Y. Pankin *et al.*, Plasma Phys. Control. Fusion **47**, 483 (2005).
[26] Xu Wei, Wan Bao-Nian and Xie Ji-Kang, Acta Phys. Sin. **52**, 1970 (2003).